Proceedings of the 17th World Congress
The International Federation of Automatic Control
Seoul, Korea, July 6-11, 2008

Plug-In Robust Compensator for a 3 DOF Piezoelectric Nanorobotic Positioner

Abdoulaye Fall, Moussa Boukhnifer, Antoine Ferreira

PRISME Institute, ENSI de Bourges, Bourges, France.
(Tel: +332 4848 4079; e-mail: antoine.ferreira@ensi-bourges.fr).

Abstract: In current AFM-based nanomanipulation systems, the commercial position closed-loop controller for piezoelectric nanopositioning stages are implemented with success in a wide range of industrial applications. Even if these controllers operate with satisfactory nominal tracking performance, considerable attention has been focused on appropriate control strategies to compensate hysteresis, nonlinearities, drift and creep for high bandwidths and large scanning regimes. As these closed-loop controllers are very cost-effective, a special interest in robust plug-in compensators seems to be a solution. We proposed in this paper a robust plug-in compensator using the H_∞ loop-shaping techniques which can be plugged into the existing controller without affecting the already satisfactory nominal tracking performance of the existing closed-loop system. Dynamic modeling, identification and robust control of a 3 d.o.f. piezoelectric nanorobotic positioner are presented in this paper in order to improve the nanorobot performance under plant parameter variations and in the presence of external disturbances. Simulation and experimental results are given to validate the proposed plug-in robust compensator in the case of a nanorobotic manipulation task.

1. INTRODUCTION

In biotechnology field, the telenanomanipulation control of microobjects (biological cells, viruses, MEMS) with human handling is difficult due to dynamics and uncertainties which are strongly impacted by the user's gesture. In applications where high performance and accuracy are not critical, constitutive nonlinearities of piezoelectric nanopositioning stages and hysteresis can be compensated by standard Proportional-Integral (PI) or Proportional-Integral-Derivative (PID) controllers. However, this can potentially lead to bandwidth limitation and inefficiencies. Even if these controllers have proved their performance, challenging problems of nanoscale control remain due to nonlinear dynamics, actuator's modeling uncertainties, instabilities and lack of robustness against external perturbations and sensor noise (Ge (1996)). As these industrial closed-loop controllers are cost-effective and dedicated, a special interest in robust plug-in compensators seems to be a solution. The key idea of this paper is to robustify existing controllers by $plug-in$ attachable robust compensators for piezoelectric nanopositioning systems. Principle of the new methods is to settle on real plants as their nominal models with local compensators. Since the additional local compensators are designed independent of previously designed controllers, they are applicable for any existing control systems including nonlinear and/or non-closed form control scheme.

A brief analysis of robust control techniques shows that a considerable number of feedback design schemes based on linear robust control techniques have been already proposed for nanopositioning systems. Development of inversion-based feedforward control with robust feedback control have proved their efficacy in output tracking in Atomic Force Microscope (Zou (2004a)), (Zou (2004b)). The performance of the inverse feedforward control, however, is strongly limited by modeling errors/uncertainties and disturbances (Devasia (2002)). Closed-loop linear H_∞ control technique seems to be an efficient alternative technique. These schemes have provided improvements in bandwidth and robustness to non linearities and hysteresis. In (Tsai (2003)), the authors proposed a Smith predictor-based H_∞ controller for a piezoactuator with an emphasis in reducing the hysteresis. In (Salapaka (2002)), a H_∞ controller design for one-dimensional nanopositioning system performing high closed-loop bandwidths and robustness against nonlinearities has been synthesized with success. Finally, a robust Glover-McFarlane H_∞ scheme (Sebastian (2003)) to simultaneously achieve performance and robustness where neither specific tracking requirement nor a characterization of uncertainty are available *a priori*.

Considering these robust control schemes, we proposed a framework for increasing the robustness of existing industrial control schemes with a quantifiable compromise on performances. We proposed in this paper a robust plug-in compensator using the H_∞ loop-shaping techniques which can be plugged into the existing controller without affecting the already satisfactory nominal tracking performance of the existing closed-loop system. A similar approach has been introduced by Salapaka in (Sebastian (2005)) where the Glover-McFarlane controller robustified a proportional double integral controller used for nano-positioning in the scanning-probe industry. In the present study, the H_∞ loop-shaping technique is applied for robustification of complex industrial controllers achieving robustness with marginal reduction in performance. Dynamic modeling, identification and robust control of a 3 degree of freedom piezoelectric nanorobotic positioner are presented in this paper in order to improve the nanorobot performance

under plant parameter variations and in the presence of external disturbances.

The paper is organized in the following way. In Section 2, a description of the nanorobotic device is given. This is followed by the frequency-domain-based system identification of the existing controller and nanorobotic positioner. The control design and the experimental results are then presented in Section 4. Experimental results are given in Section 5 to validate the proposed plug-in robust compensator in the case of a nanorobotic manipulation task.

2. PIEZOELECTRIC NANOROBOTIC POSITIONER DESCRIPTION

The nanomanipulator structure is composed of three linear translation stages (x,y,z) driven by DC motors for coarse motion (range: 8 mm, accuracy: 15 nm) combined with a 3 d.o.f ultra-high-resolution piezomanipulator (x,y,z) for fine positioning (range: 100 μm, accuracy: 1 nm). This hybrid nanopositioning system combines the advantages of ultra-low inertia, high-speed and long travel range (Fig.1(a)). The micro-endeffector is constituted by a piezoresistive AFM cantilever integrating a full-bridge strain gauge sensors ((Fig.1(b)).

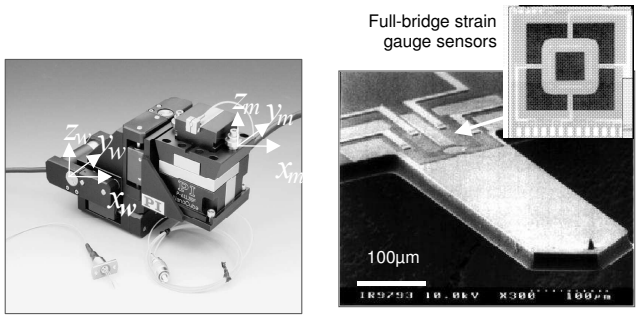

Fig. 1. Structure of the hybrid 6 dof AFM-based nanomanipulator and its sensorized force cantilever.

The 3 d.o.f ultra-high-resolution piezomanipulator (P-611.3S NanoCube from Physics Instruments) is a versatile, multi-axis piezo-nanopositioning system. Its 100x100x 00 μm positioning and scanning range comes in an extremely compact package. Equipped with a zero-stiction, zero-friction guiding system, this piezomanipulator provides motion with ultra-high resolution and settling times of only a few milliseconds. Single-axis nanopositioning stage with anti-accurate-motion flexure design. The best flexure designs provide guiding precision in the low nanometer range. In open-loop operation, the platform's position is roughly proportional to the drive voltage. In the closed-loop version, the Proportional-Integral (PI) controller allows absolute position control. However, existing closed-loop controller is designed to achieve specific tracking and performance requirements (such as zero steady-state tracking) in a narrow frequency closed-loop bandwidth. During nanomanipulation tasks, the x-y-z nanopositioner servo-controller lacks in robustness against:

a) Modeling uncertainties:

(1) Mechanical nonlinearities of mechanical-guiding systems for large travel ranges;
(2) Modeling uncertainties due to operating point, temperature effects and time execution;
(3) Hysteresis and creep effects due to piezoelectric ceramics.

b) External perturbations:

(1) Noise measurement perturbations;
(2) Force/torque perturbations during nanomanipulation.

Considering these limitations, we proposed in the following a robust plug-in compensator using the H_∞ loop-shaping technique which can be plugged into the existing PI-controller without affecting the already satisfactory nominal tracking performance.

3. IDENTIFICATION

The digital system to be identified is constituted of both components: the piezoelectric nanopositioner and the PI-controller embedded into the acquisition card. The acquisition board is composed of digital inputs (DAC) and outputs (ADC), the identification should be considered as a discrete system. Among the various modes of identification for numerical systems (Longchamp (2006)) (Rivoire (1992)), we choose the least squares simple method. This choice is justified by the simplicity of the method during implementation, accuracy of the identified parameters and off-line parameters adjustment. The least square method is based on the determination of a vector of parameters so as to minimize a error vector ϵ. It consists to minimize the square of the euclidian norm of the error vector. The function :

$$J : R^p \rightarrow R \tag{1}$$

to minimize is defined by:

$$J(\vartheta) = \| \varepsilon(k) \|^2 = \varepsilon^T(k)\varepsilon(k) = (y(k) - \phi(k)\vartheta)^T(y(k) - \phi(k)\vartheta) \tag{2}$$

The vector parameters minimizing the criterion $J(\vartheta)$, denoted $\widehat{\vartheta}(k)$, is called the estimated vector parameters defined by (Rivoire (1992)):

$$\widehat{\vartheta}(k) = (\phi^T(k)\phi(k))^{-1}\phi^T(k)y(k) \tag{3}$$

where $\phi(k)$ is the observation matrix $\phi(k)$ of p-order.

In to order identify the wide dynamics bandwidth of the servo-nanopositioner, we choose a Pseudo-Random Pattern Generator signal (PRPG). It has been already proved reliable for a good identification in different dynamic systems.

The scheme of Fig.2 depicts the principle of the numerical identification. $U(Z)$ represents the numerical input signal (PRPG input signal), $Y(Z)$ the numerical output signal of the system. The system is provided with analog-to-digital (ADC) and digital-to-analog (DAC) converters. It offers the possibility to convert discrete-to-continuous and continuous-to-discrete space.

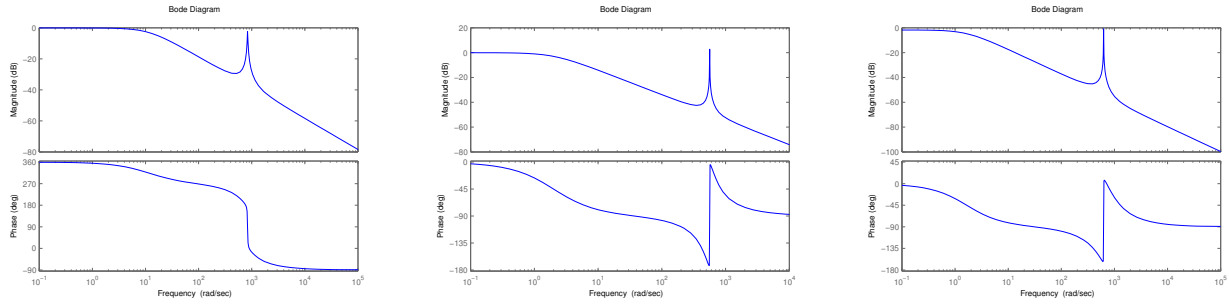

(a) (b) (c)

Fig. 3. Experimental frequency responses of (a) x-axis, (b) y-axis and (c) z-axis.

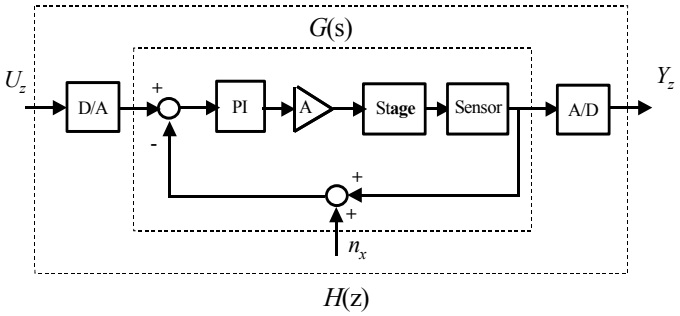

Fig. 2. Identification of the system transfer function.

In Fig.2, the terms $G(S)$ and $H(z)$ represent the transfer functions of the continuous system and the discrete system, respectively. The parameters provided by the identification represent the a_i and the b_j of the discrete transfer function which is given by the following expression:

$$\frac{b_0 z^2 + b_1 z + b_2}{z^3 + a_1 z^2 + a_2 z + a_3} \tag{4}$$

The identification was carried out for several operating points, ranging from $0\mu m$ to $60\mu m$ with elementary steps of $10\mu m$ and driving frequencies lower than the resonance frequencies. The discrete models have been identified with averaged parameter values for x, y and z axes, respectively:

$$H_x(z) = \frac{0.00535z^2 + 0.0271z + 0.0507}{z^3 - 0.00557z^2 + 0.0196z - 0.93} \tag{5}$$

$$H_y(z) = \frac{0.003z^2 + 0.00741z + 0.0117}{z^3 - 0.00579z^2 + 0.025z - 0.997} \tag{6}$$

$$H_z(z) = \frac{0.000556z^2 + 0.00535z + 0.00761}{z^3 - 0.00566z^2 + 0.0222z - 1} \tag{7}$$

Then, we used the MATLAB function $d2c$ to convert discrete-to-continuous functions:

$$H_x(s) = \frac{12s^2 - 1.106 \times 10^4 s + 8.045 \times 10^6}{s^3 + 29.03s^2 + 6.971 \times 10^5 s + 8.13 \times 10^6} \tag{8}$$

$$H_y(s) = \frac{1.967s^2 - 926.4s + 6.371 \times 10^5}{s^3 + 0.812s^2 + 3.177 \times 10^5 s + 6.399 \times 10^5} \tag{9}$$

$$H_z(s) = \frac{1.038s^2 - 924.7s + 5.32 \times 10^5}{s^3 + 9.979 \times 10^{-13} s^2 + 3.918 \times 10^5 s + 6.51 \times 10^5} \tag{10}$$

The results presented in Fig.3 show the experimental frequency responses. Fig.4 compares the step responses and PRPG obtained from theory and experiments along the x-axis. In both cases, the results show good tracking performances with negligible error.

However, it should be noticed that the identified models vary strongly due to uncertain dynamics and are subject to modeling uncertainties. It can be explained by the following reasons:

- Time-varying changes in flexure stages stiffness are due to repeated cycling at different strains (uncertain pole location).
- Unmodeled nonlinear effects are significant (stiffness is nonlinear versus position).
- Variance of the stage dynamics due to diverse operating conditions.
- Frequency response at the same operating point varies with time. It typically manifests itself as a change in resonance locations.
- Temperature variation affects directly the parameters of piezoelectric ceramics.

4. PLUG-IN ROBUST CONTROLLER DESIGN

The existing controller is a proportional integral (PI) and for the robustification of the existing controller we use the H_∞ loop shaping technique. In this part, we will present the principles of the H_∞ loop shaping control and how it can be integrated in a robust plug-in controller.

4.1 H_∞ Standard Problem

For $P(s)$ and $\gamma > 0$ are given, the H_∞ standard problem of is to find $K(s)$ which:

- Stabilize with way internal loop system in the Fig.5
- Maintain the norm with $F_L(P, K)$ defined as the transfer function of exits Z according to the entries W.

4.2 Coprime Factorization Approach

An approach was developed by (Glover (1988)) and (Glover (1989)) starting from the concept of the coprime

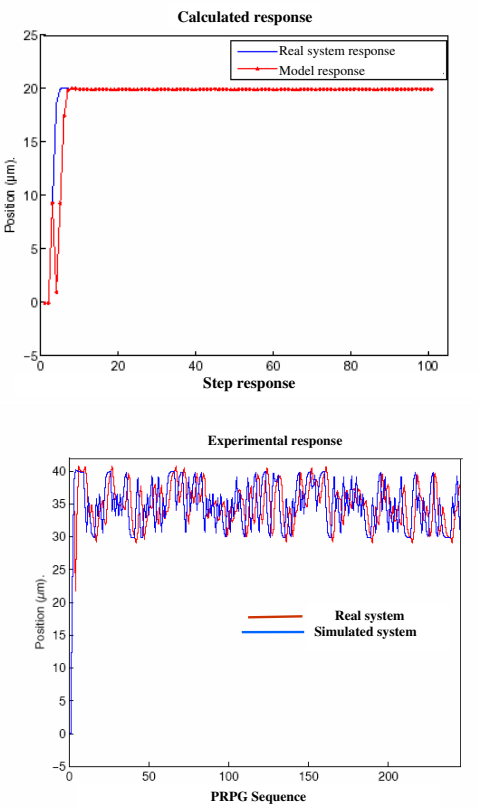

Fig. 4. Experimental responses (red lines) are compared with the responses of the models (blue lines) $H_x(s)$.

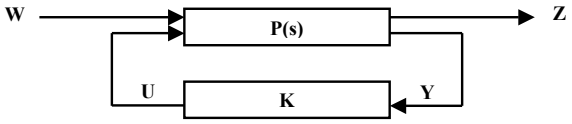

Fig. 5. H_∞ standard problem.

factorization of transfer matrix. This approach presents interesting properties and its implementation calls upon notions traditional of automatic control.

4.3 Robust Controller Design using Normalized Coprime Factor

We define the nominal model of the system to be controlled starting from the coprime factors on the left: $G(s) = \widetilde{M}(s)^{-1}\widetilde{N}(s)$. Then a perturbed model is written (see Fig .6).

$$\widetilde{G} = (\widetilde{M} + \Delta_m)^{-1}(\widetilde{N} + \Delta_n) \tag{11}$$

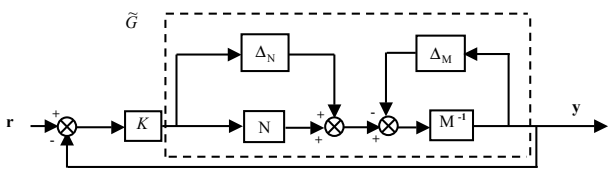

Fig. 6. Coprime factor robust stabilization problem.

where $\widetilde{G}$ is a left coprime factorization (LCF) of G, and Δ_m, Δ_n are unknown and stable transfer functions representing the uncertainty. We can then define a family of models with the following expression :

$$\xi_\epsilon = \{\widetilde{G} = (\widetilde{M} + \Delta_m)^{-1}(\widetilde{N} + \Delta_n) : \|(\Delta_m \quad \Delta_n)\|_\infty < \epsilon\} \tag{12}$$

where ϵ_{max} represent the margin of maximum stability. The robust problem of stability is thus to find the greatest value of $\epsilon = \epsilon_{max}$, such as all the models belonging to ξ_ϵ can be stabilized by the same corrector K. The problem of robust stability H_∞ amounts finding γ_{min} and $K(s)$ stabilizing $G(s)$ such as:

$$\left\| \begin{pmatrix} I \\ K \end{pmatrix} (I - GK)^{-1} (I \quad W_2 G W_1) \right\|_\infty = \gamma_{min}^{-1} = \epsilon_{max}^{-1} \tag{13}$$

However, Mc Farlane (1992) showed that the minimal value γ of is given by:

$$\gamma_{min} = \epsilon_{max}^{-1} = \sqrt{1 + \lambda_{sup}(XY)} \tag{14}$$

where λ_{sup} indicates the greatest eigenvalue of XY. Moreover, for any value $\epsilon < \epsilon_{max}$ a corrector stabilizing all the models belonging to ξ_ϵ is given by:

$$\begin{aligned} K(s) &= B^T X (sI - A + BB^T X - \gamma^2 ZYC^T C)^{-1} \gamma^2 ZYC^T \\ Z &= (I + YX - \gamma^2 I)^{-1} \\ \gamma &= \epsilon^{-1} \end{aligned} \tag{15}$$

where A, B and C are state matrices of the system defined by the function G and X, Y are the positive definite matrices and solution of the Ricatti equation :

$$A^T X + XA - XBB^T + C^T C = 0 \tag{16}$$

$$AY + YA^T - XC^T C + BB^T = 0 \tag{17}$$

4.4 The Loop Shaping Design Procedure

Contrary to the approach of Glover-Doyle, no weight function can be introduced into the problem. The adjustment of the performances is obtained by affecting an open modeling (*Loop Shaping*) process before calculating the compenstor. The design procedure is as follows :

- We add to the matrix $G(s)$ of the system to be controlled a pre-compensator W_1 and/or a post-compensator W_2, the singular values of the nominal plant are shaped to give a desired open-loop shape. The nominal plant $G(s)$ and shaping functions W_1 and W_2 are combined in order to improve the performances of the system such as $G_a(s) = W_2(s)G(s)W_1(s)$ (see Fig.7.a). In the monovariable case, this step is carried out by controlling the gain and the phase of $G_a(jw)$ in the Bode plan.
- From coprime factorizations of $G_a(s)$, we apply the previous results to calculate ϵ_{max}, and then synthesize

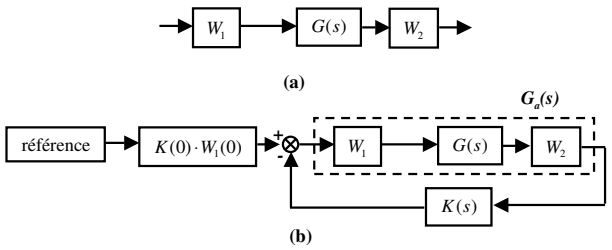

Fig. 7. Loop Shaping design procedure.

a stabilizing controller K ensuring a value of ϵ slightly lower than ϵ_{max}.

$$\left\| \begin{pmatrix} I \\ K \end{pmatrix} (I - W_2 G W_1 K)^{-1} (I \quad W_2 G W_1) \right\|_\infty = \gamma = \epsilon^{-1} \tag{18}$$

- The final feedback controller is obtained by combining the H_∞ controller K with the shaping functions W_1 and W_2 such that $G_a(s) = \mathrm{W}_2(s)G(s)W_1(s)$ (See Fig.7.b).

5. APPLICATION TO THE PIEZOELECTRIC NANOPOSITIONER

5.1 Implementation of the Controllers

In this part, we explain the synthesis and implementation of the controllers. The synthesis of the controller K is obtained according to the implementation shown in the Fig.7 using the command $ncfsyn$ of MATLAB -Analysis and Synthesis toolbox (Balas (1994)). The controller K is obtained by combining the pre-filter and the post-filter. The pre-filter and post-filter are used to shape the open-loop plant to achieve a desired frequency responses according to some well defined design specifications such as bandwidth and steady-state error (Lundstrom (1991)). To obtain a high gain at low frequency, a PI controller is synthesized for the x-axis like pre-filter W_1 and in order to obtain a small gain at high frequency, a low-pass filter is synthesized like pre-filter W_2. In order to obtain a high performance and a good robustness, we add the following weight functions:

$W_1 = 50 \times \frac{10s+35.2}{10s}, W_2 = \frac{1}{s+11.3}$.

Using these weight functions, we obtained a six-order H_∞ controller. In order to implement this controller, we use the MATLAB function *balmr* to reduce the controller order to the third-order approximation. The resultant $plug-in$ robust controller is given by :

$$K_r(s) = \frac{-72.69s^2 - 1824s - 6706}{s^3 + 66.88s^2 + 625.7s - 5.07 \times 10^{-11}}. \tag{19}$$

and the discrete controller :

$$K_{r_d}(s) = \frac{0.1726z^2 - 0.3347z + 0.1622}{z^3 - 2.842z^2 + 2.688z - 0.846} \tag{20}$$

5.2 Characterization of the Nanopositioning Device

In this section, the nanopositioning is characterized in terms of range, sensitivity and resolution in the open- and closed-loop configurations. The calibration data showed some hysteresis in open-loop. Hysteresis is primarily due to the nonlinear relationship between applied voltage and displacement which are important for large deflections. To present the effectiveness of the H_∞ closed-loop design, the hysteresis curves obtained in open-loop (Fig.8.a) are compared with the closed-loop design using the H_∞ controller (Fig.8.b). We can see clearly that for a nanopositioning displacement of 40 μ m a maximum output hysteresis of 10 μ m was observed. The same experiment with the closed-loop controller showed that the effects were practically eliminated. An important observation comes from the fact that the operating applied voltage is settled to $100V$ while the system was identified for a low value of input signal (PRPG signal). It shows clearly the linearity relationship between the input-output signals. Similar linearity results have been measured when considering creep effects. It should be noticed that important differences were observed for different displacement with PI and H_∞ controller. High precision is obtained with robustified PI controller.

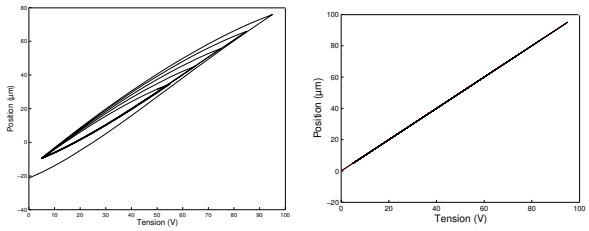

(a) (b)

Fig. 8. Hysteresis in open-loop and closed-loop H_∞ controller.

5.3 Experimentation in nanopositioning tasks

The set of experiments of Fig.9 shows the step responses with the simple PI controller and the H_∞ $plug-in$ robust controller. The experimental results demonstrate the excellent position tracking with the proposed robust controller. The position output tracks perfectly the position reference. It should be noticed when considering PRPG signals, the experimental results shows a good compromise between performances and robustness with the robustified PI controller (Fig.10). The proposed $plug-in$ robust controller design ensures the robust stability against strong disturbances, the experimental response with a step perturbation demonstrate the excellent tracking and the position follows well the reference. We noticed that the response is not affected by the application of a step disturbance (Fig.11.a) or a noise perturbation (Fig.11.b).

6. CONCLUSION

The Loop Shaping Design Procedure (LSDP) using H_∞ synthesis has been applied for robustified controller design of nanopositioning system. In the proposed H_∞ loop shaping design procedure, the model uncertainties are included as perturbations to the nominal model, and robustness is guaranted by ensuring that the stability

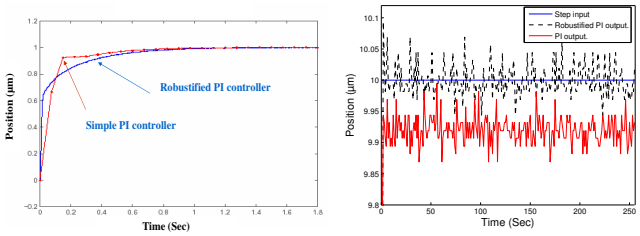

(a) (b)

Fig. 9. (a) Step responses for PI and H_∞ controllers and (b) corresponding static errors.

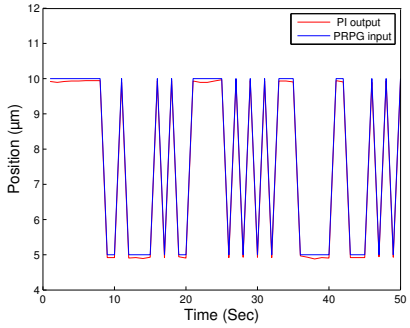

(a)

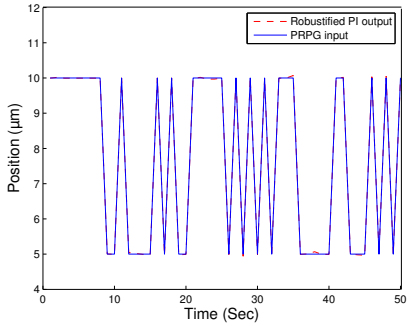

(b)

Fig. 10. PRPG responses with (a) PI controller (b) robustified PI controller.

specifications (nanometer resolution) are satisfied in the worst-case uncertainty. As conclusion, a very good point of the design is the remarkable features that achieves robustness with marginal reduction of performance.

REFERENCES

P. Ge, M. Jouaneh Tracking control of a piezoceramic actuator. *IEEE Trans. on Control Systems Technology*, Vol.4, No.3, pages 209–216, 1996.

Q. Zou, K.K. Leang, E. Sadoun, M.J. Reed, S. Devasia Control issues in high-speed AFM for biological applications: Collagen imaging example. *Asian Journal Control,*, Vol.8, pages 164–178, 2004.

Q. Zou, S. Devasia Preview-based optimal inversion for output tracking: Application to scanning tunneling microscopy. *IEEE Trans. on Control Systems Technology*, Vol.12, pages 375–386, 2004.

S. Devasia Should model-based inverse input be used as feedforward under plant uncertainty. *IEEE Trans. on Automatic Control,*, Vol.47, pages 1865–1871, 2002.

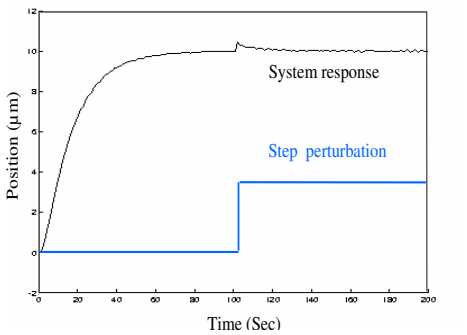

(a)

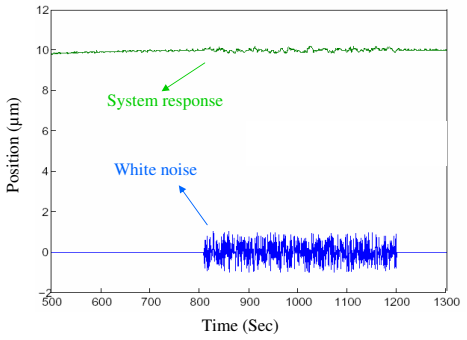

(b)

Fig. 11. Step responses with robustified PI controller in presence of (a) step perturbation (b) white noise.

M. Tsai, J. Chen Robust Tracking control of a piezoactuator using a new approximative hysteresis model. *J. of Dynamics Systems, Measurement and Control*, Vol.125, pages 96–102, 2003.

S. Salapaka, A. Sebastian, J. P. Cleveland, V. Salapaka High bandwidth nano-positioner: a robust control approach. *Review of Scientific Instruments*, Vol.73, No.9, pages 3232–3241, 2002.

A. Sebastian, S. M. Salapaka H_∞ loop shaping design for nanopositioning. *ACC*, Denver, pages 3708–3713, 2003.

A. Sebastian, S. M. Salapaka Design Methodologies for Robust Nano-Positioning. *IEEE Trans. on Control Systems Technology*, Vol.13, No.6, pages 868–876, 2005.

R. Longchamp Commande numrique de systmes dynamiques, *Presse polytechnique*, Lausanne 2006.

M. Rivoire, J.-L. Ferrier, Cours d'automatique Tome 3, "Commande par calculateur", 1992.

K. Glover, D. Mc Farlane, Robust stabilization of normalized coprime factors: An explicit H_∞ solution, *IEEE ACC*, Atlanta, GA, 1988.

K. Glover, D. Mc FArlane, Robust Stabilization of normalized coprime factor plant descriptions with H_∞ bounded uncertainly, *IEEE Trans. on Automatic Control*, Vol.34, pp.821-830, 1989.

D. Mc Farlane, K. Glover A Loop Shaping design procedure using H_∞ synthesis, *IEEE Trans. on Automatic Control*, Vol 37, pp.759-769, 1992.

G.J. Balas, J.C. Doyle, K. Glover, A. Packard, and R. Smith, $\mu-$ Analysis and Synthesis Toolbox, Natick, MA: *The MathWorks*, Inc, 1994.

P. Lundstrom, S. Skogstad, Z.C. Wang, Weight selection for H_∞ and $\mu-$control methods: insights and examples from process control, *Workshop on H_∞ Control*, Brighton, U.K., pp.pp.139-1991, 1991.